PAPER • OPEN ACCESS

Stability modeling of complex underground mine openings integrating point clouds and FEM 3D

To cite this article: F Agliardi *et al* 2021 *IOP Conf. Ser.: Earth Environ. Sci.* **833** 012108

Stability modeling of complex underground mine openings integrating point clouds and FEM 3D

F Agliardi [1,2], R Castellanza [1,2], G Frigerio [2] and G M Orlandi [3]

[1] University of Milano-Bicocca, Earth and Environmental Sciences, Milano, Italy
[2] EG4 Risk s.r.l., Milano, Italy
[3] Studio Associato di Geologia Spada, Bergamo, Italy

federico.agliardi@unimib.it

Abstract. The stability analysis of underground mine systems with complex 3D geometry is still a challenging task, especially when abandoned mines are planned for new uses with public access, that imply more restrictive safety requirements. This inherently multi-scale problem requires both the evaluation of the global mine stability and the assessment of local deformation and failure mechanisms of individual pillars or roof sectors in a robust 3D modeling framework. We integrated 3D remote survey techniques and FEM 3D modeling to perform a comprehensive stability analysis of an abandoned fluorite mine system in the central Southern Alps (Italy), including ten levels excavated in bedded limestones. We reconstructed the 3D geometry of three levels undergoing a reuse plan, combining a dynamic LiDAR system and close-range photogrammetry. We used point clouds in a workflow to generate solids, excavate the 3D analysis domain and generate a FEM 3D mesh for numerical modeling. We performed a series of continuum-based FEM 3D simulations of mine excavation and rock mass strength degradation. Our results allowed assessing the global stability of the abandoned mine and identifying critically stressed roof sectors and pillars to prioritize the local-scale analysis, remediation and monitoring of critical spots.

1. Introduction

Abandoned mines are increasingly recognized as valuable assets that can be reused in different ways, including civil uses (e.g. commercial, recreational or educational) or storage of different types of goods (e.g. food), waste or resources as oil and water [1]. Nevertheless, abandoned mines can undergo progressive decrease of stability conditions due to chemical weathering, progressive rock damage accumulation and uncontrolled variations of groundwater regime, constrained by geological and environmental conditions. These processes can result in subsidence, flooding or catastrophic failure threatening life, properties, and the environment [2,3]. Moreover, civil reuse of former mining voids has increased safety requirements with respect to active mining environments and must be supported by suitable design and monitoring measures. Dealing with abandoned mines requires a robust assessment of the stability conditions of underground structures, considering the site-specific geological conditions and mining layouts, yet it remains a difficult task.

Mine openings can undergo deformation and failure processes on both the global and local scales (e.g. affecting specific roof sectors or pillars). Local scale failure can either promote global instability or hamper the suitability of the mine sectors for specific uses. Challenges in mine stability analysis include accounting for: a) the complexity and heterogeneity of rock mass constitutive behaviors, that

IOP Conf. Series: Earth and Environmental Science **833** (2021) 012108 doi:10.1088/1755-1315/833/1/012108

control the style and time-dependency of failure processes [4]; b) structural controls exerted by rock mass fabric and individual structures [5]; and c) the effects of complex 3D void geometries on stress concentration and damage localization [6]. Advanced developments in numerical modeling of underground mines have been proposed in the last decades, accounting for the effects of local geology, rock properties and fracturing in different stress conditions [4,5,7]. Nevertheless, stability modeling in complex geometrical and geological conditions has mainly been dealt with in 2D [8], while 3D applications to multi-level mine systems with irregular geometries are usually based on simplified void and pillar geometries [9,10,11].

In this work we integrated different remote survey techniques and a FEM 3D modeling approach to perform an accurate stability analysis of an abandoned fluorite mine in complex geometrical and geological conditions, accounting for both global- and pillar-scale stability.

2. The Dossena underground mine system

The Dossena fluorite mine system (Lat: 45°53’46’’N; Lon: 9°40’56’’E) is located in the Orobic Alps (central Southern Alps, Italy), and includes over 20km of mining voids organized in ten NW-SE trending levels connected by inclined tunnels. Mining activity started in 1930s and was abandoned in 1981. Most of the mine was excavated in bedded limestones of the Breno Fm., characterized by a rather constant orientation (230/25) and the occurrence of up to 6m thick lenticular fluorite mineralizations parallel to the sedimentary bedding. Mining was performed by excavating tunnels and rooms with irregular geometry, constrained by limestone beds up to 2.5m thick. Rooms are supported by vertical or inclined pillars up to 5m high and connected by haulage ways with regular cross-sections and frequent lateral headings (figure 1).

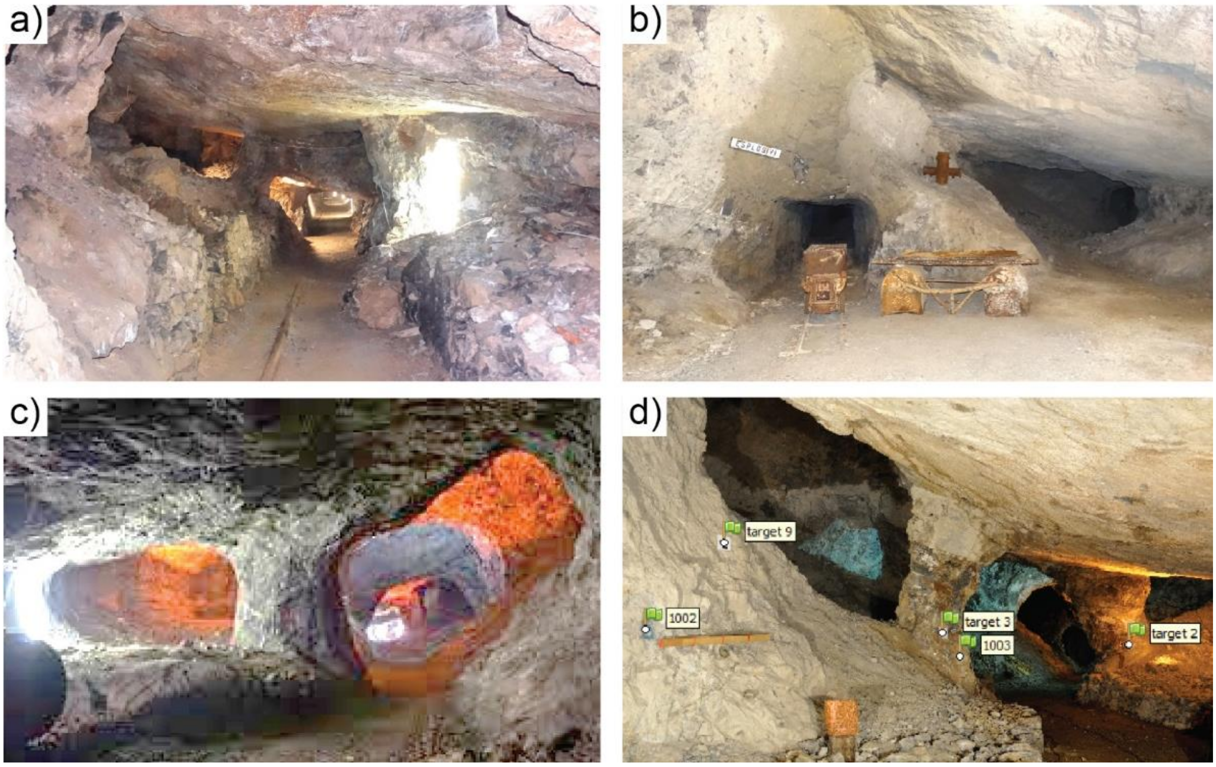

Figure 1. Complex mining voids at the Dossena mine. 4m wide haulage ways driven along sedimentary bedding with irregular lateral headers (a); large rooms, up to 20 m wide (b), with trapezoidal cross section supported by vertical (c) or inclined pillars (d). Coded targets and scale bars used as reference for close-range photogrammetric surveys are visible in inset (d).

IOP Conf. Series: Earth and Environmental Science **833** (2021) 012108 doi:10.1088/1755-1315/833/1/012108

In the last few years, a rehabilitation project supported by the local community was developed to exploit abandoned underground spaces of the Dossena mine system for civil reuse. This includes cultural visits, recreational activities, and an underground research laboratory. The project involves three mining levels connected by a narrow descendery with an inclination of 15° (figure 4), namely:

- upper level (1021-1023 m asl): accessed through the mine main entrance by a 100m long haulage way surrounded by narrow adits. To the SE, the level is up to 35 m deep below the topography and made of five rooms up to 20m wide and 8m high, supported by pillars.
- intermediate level (1011 m asl): located below and to the SW with respect to the upper level and including a 170m long network of small irregular rooms and narrow tunnels and headings.
- lower level (996-999 m asl): located at the bottom of the studied mine sector and made of a 70m long irregular cavity, up to 10m wide and 12m high, with lateral adits and headings and connected to a secondary mine exit through a wide room supported by roof pillars.

3. Rock mass characterization

We characterized rock properties through laboratory tests on 40 limestone samples, including Brazilian, uniaxal compressive strength and multistage triaxial tests. These allowed determining intact rock strength, elastic properties (table 1) and complete stress-strain curves. Limestones hosting the mine have high strength and average modulus ratio with a distinct brittle behavior.

We upscaled rock properties to the fractured rock mass conditions in a Hoek-Brown framework [12]. Discontinuity surveys were carried out in the field and on point clouds (figure 2) to identify and characterize fractures sets in terms of orientation, spacing statistics, and frictional properties. These data allowed well-constrained estimates of the Geological Strength Index, required to upscale intact rock properties to an "equivalent continuum" rock mass. Rock mass structure is fairly homogeneous in the entire considered domain of the mining system, with 3 main discontinuity sets including bedding (modal orientation: 230/25; spacing in the range 20-60 cm and up to 250 cm), 2 joint sets (modal orientations: 185/89 and 246/89; spacings in the range 10-40 cm) and undisturbed GSI values in the range 50-60.

Table 1. Rock mass properties. m_i, m_b, s and a are Hoek-Brown failure criterion parameters.

Intact rock				
Uniaxial compressive strength (UCS, MPa)	121			
Young modulus (Et_{50}, MPa)	28000			
m_i	10			
Rock mass				
Geological Strength Index (GSI)	55	45	40	35
D	0	0	0	0
m_b	2.005	1.402	1.173	0.981
s	0.0067	0.002	0.0012	0.0007
a	0.500	0.508	0.511	0.515
Angle of dilatancy (ψ, °)	3	3	3	3
Uniaxial compressive strength (σ_c, MPa)	9.70	5.40	3.99	2.90
Mass strength (σ_{cm}, MPa)	23.50	18.85	16.86	15.00
Tensile strength (σ_t, MPa)	0.41	0.19	0.13	0.09

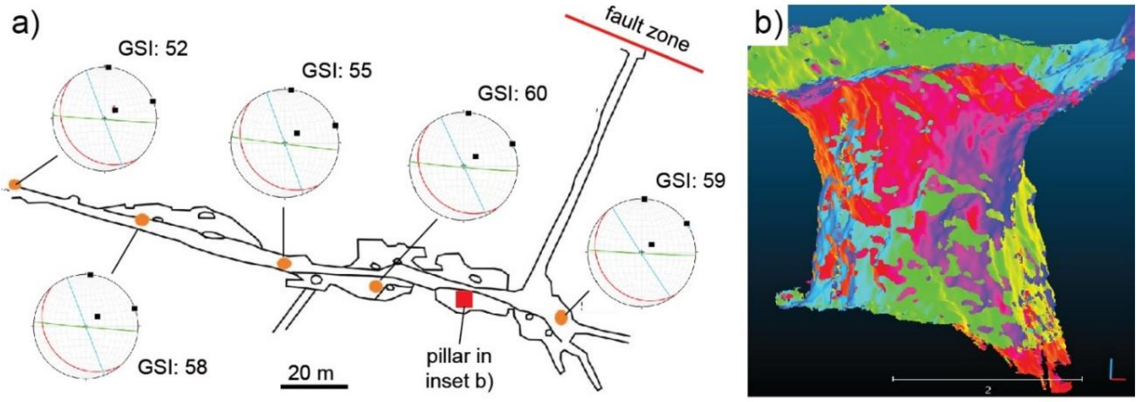

Figure 2. Rock mass characterization. a) standard discontinuity survey stations, related stereoplots of fracture sets (modal plane, great circles) and GSI values. b) virtual discontinuity survey performed on high-resolution photogrammetric point cloud (colour: dip direction).

4. 3D geometrical model: from point cloud to FEM mesh

4.1. 3D surveys

An accurate representation of the 3D geometrical and geomechanical complexity of underground structures is key to a reliable assessment of mine stability. Nevertheless, it is still challenging due to extreme mine void complexity, limited accessibility and environmental survey conditions [13,14]. In this context, we performed a multi-scale, high resolution geometrical reconstruction of the analysis domain exploiting the potential of different 3D survey techniques.

We used close-range Structure-from-Motion (SfM) photogrammetry to reconstruct the 3D geometry of individual rooms and pillars with mm-scale accuracy. We carried out 13 survey projects using a 12-megapixel DSLR camera mounted on tripod. More than 1500 pictures were shot in underground conditions, assisted by 500W halogen spotlights and using 12-bit coded targets, scalebars and benchmarks as references for processing optimization and model registration. To allow for co-registration and absolute geo-referencing of different SfM models, we established a topographic network based on total station survey of 43 Ground Control Points, linked to a DGPS reference station established outside the mine. SfM processing, performed using the software Agisoft Metashape™, provided point clouds with a spatial accuracy in the range 0.7-3mm and an absolute RMS error lower that 4 cm. Point clouds have native RGB attributes allowing the reconstruction of Digital Outcrop Models (figure 3a) suitable for geological analysis and virtual discontinuity survey (figure 2b).

On the other hand, photogrammetric surveys are unable to cover the entire system of mining voids, due to limited accessibility hampering suitable survey layouts in very narrow or complex voids (e.g. intermediate mining level). Moreover, the accuracy of point clouds derived from close-range photogrammetry usually exceeds the requirements of an effective 3D geometrical reconstruction for numerical model meshing. Thus, to characterize the entire void system in a realistic yet effective way, we carried out a complete survey using a Gexcel Heron MS-1™ mobile laser scanner. It is based on a SLAM technology combining a laser scanner and an inertial measurement unit (IMU), capable of acquiring 700000 point measurements per second with an accuracy of about 2 cm. A total path of 1255 m was surveyed in about 2 hours, resulting in a point cloud of the mining system with an average surface point density of about 6000 points/dm^2 (figure 3b).

4.2. 3D solid model

We processed point clouds obtained by 3D surveys to generate a geometrical model optimized for numerical modeling accuracy and computational efficiency. An accurate sub-meter description of the geometry of pillars, roof sectors and small voids is required to simulate stress distribution and concentrations in numerical modeling. On the other hand, excessive geometrical complexity can hamper the generation of 3D finite element meshes or result in unacceptable computation time, due to the occurrence of many small finite elements around tiny geometrical irregularities.

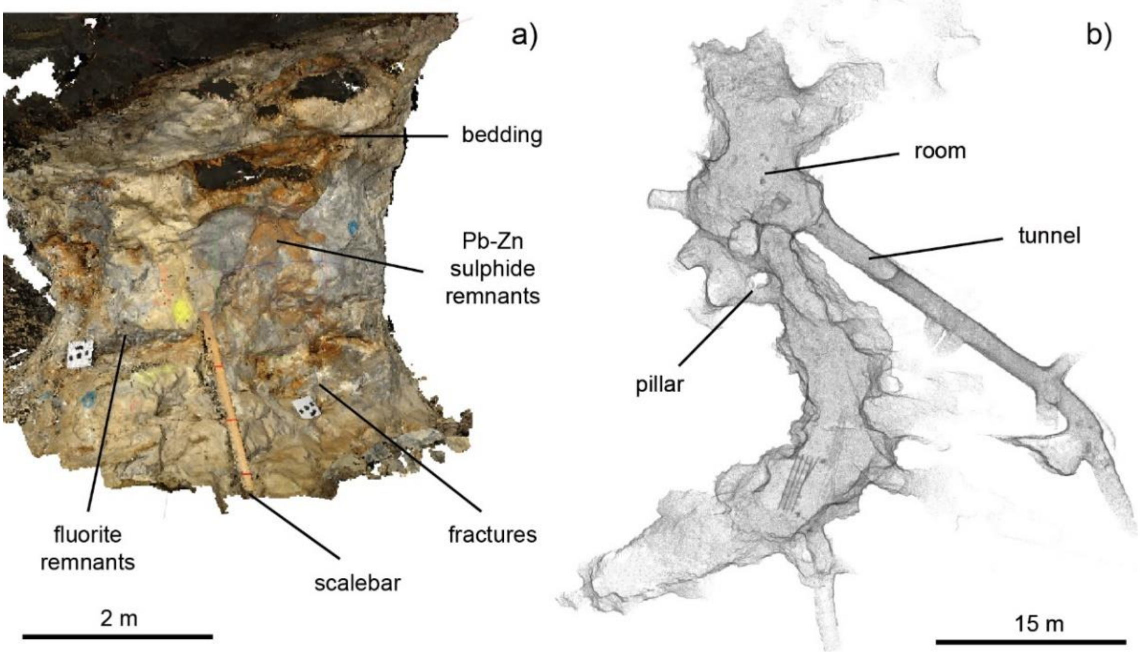

Figure 3. Examples of point clouds derived from different 3D survey techniques. a) close-range photogrammetric model of a pillar (mm-scale accuracy, RGB); b) point cloud acquired using a mobile laser scanner (cm-scale accuracy, no RGB; courtesy Gexcel s.r.l.).

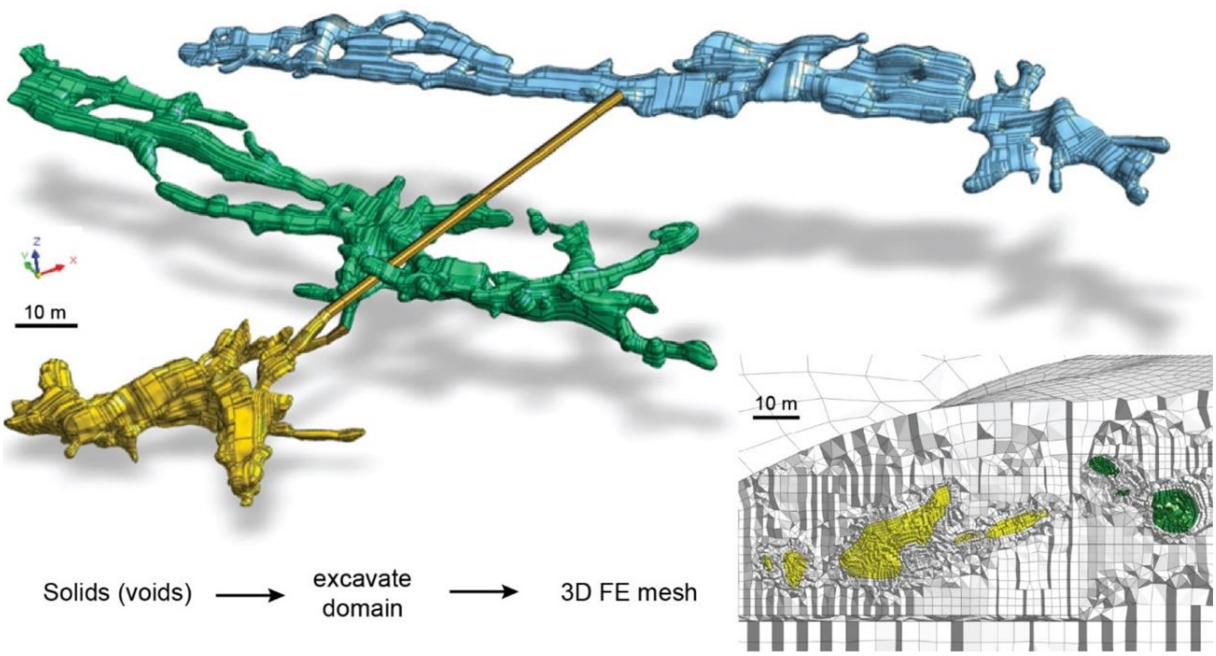

Figure 4. 3D reconstruction of the considered sector of the mine system, including three levels and an inclined connecting tunnel. Solids representing voids are used to excavate the 3D model domain, later discretized into a non-homogeneous 3D finite element mesh.

To obtain an accurate and smooth representation of different elements of the mining systems characterized by different size (i.e. rooms, pillars, haulage ways, headings), we processed point clouds in a workflow including: a) point cloud cleaning, e.g. removal of isolated points and points representing foreign objects; b) semi-automatic filtering (decimation, homogenization, smoothing); c) manual point cloud repair (e.g. hole filling), merging and fine registration.

The processed point cloud model allowed reconstructing a solid model representing the network of mining voids (figure 4). This was used to excavate a modeling domain with a planimetric area of 350x380 m, limited above by the topography (extracted from a Digital Elevation Model with cell size of 5 m) and extending 50 m deeper than the bottom of the mining voids (figure 4). The resulting solid provided a very accurate representation of the smaller object of interest (e.g. pillars, small cavities) to support the generation of 3D finite-element meshes suitable for reliable numerical analysis yet avoiding geometrical artifacts resulting by excessive point cloud details.

5. 3D finite element modeling

5.1. Model setup

We performed a series of 3D, continuum-based, non-linear FEM numerical analyses using the MIDAS GTS-NX^{TM} code. The analysis domain was discretized into a FEM 3D mesh consisting of 1530000 hybrid finite elements (hexa-, penta- and tetrahedral) with size progressively variable between 0.5 m (close to voids) and 10 m (external boundaries). Close to the topographic surface, finite elements had an average size of 3 m. Boundary conditions were imposed by preventing horizontal displacements at lateral boundaries and fixing both horizontal and vertical displacements at the bottom boundary. We considered a homogeneous material characterized by an elastoplastic behaviour according to a Hoek-Brown failure criterion with post-peak dilatancy. Rock mass properties have been estimated combining laboratory and field data for different GSI values of 55, 45, 40 and 35, respectively (table 1). These were considered as rock mass degradation scenarios for a shear strength reduction numerical stability analysis [15], aimed at identifying potential failure mechanisms and evaluating associate "factors of safety" (i.e. critical strength reduction factors).

We performed numerical simulations in different steps, namely: a) initialization of a gravitational stress field within the model domain without excavations, to simulate undisturbed, pre-mining stress distributions; b) excavation of the mine system with mechanical properties corresponding to actual rock mass conditions (GSI=55), to represent present-day stress-strain distributions and outline critical spots undergoing irreversible (plastic) strain; c) staged reduction of rock mass properties (lower GSI values) to identify potential local and global failure mechanisms and estimate related factors of safety.

5.2. Model results: global and pillar stability

Simulations revealed steeply dipping major principal stress concentrated within localized roof sectors and the pillars of the upper mining level, with maximum values reaching 8 MPa (figure 5a). Less intense stress concentrations also occurred at localized spots of the intermediate and lower sectors. In actual conditions, plasticity indicators only revealed localized yielding within upper level pillars characterized by complex geometry, e.g. inclined or irregular (figure 5b). Strength reduction resulted in irregularly distributed yielding of roofs and pillars sectors in all mining levels. However, failure mechanisms were always local and controlled by small-scale 3D geometry. Global stability was satisfied until a degradation to GSI=35, corresponding to a numerical factor of safety exceeding 3.

The average stress state within individual pillars was difficult to quantify, due to their geometrical complexity and the variable conditions of surrounding voids (figure 6). Nevertheless, our results provided credible estimates of the maximum values of the major principal stresses, that reached 6-7 MPa in the upper level, 3-4 in the intermediate level, and 2-3 in the lower level. Considering reference values of mass strength in the Hoek-Brown framework (σ_{cm}, table 1) and using the method proposed by Obert and Duvall [16], we estimated pillar factors of safety ranging between 3.3 (GSI=55) and 2.1 (GSI=35) in the most unfavorable conditions of the upper level.

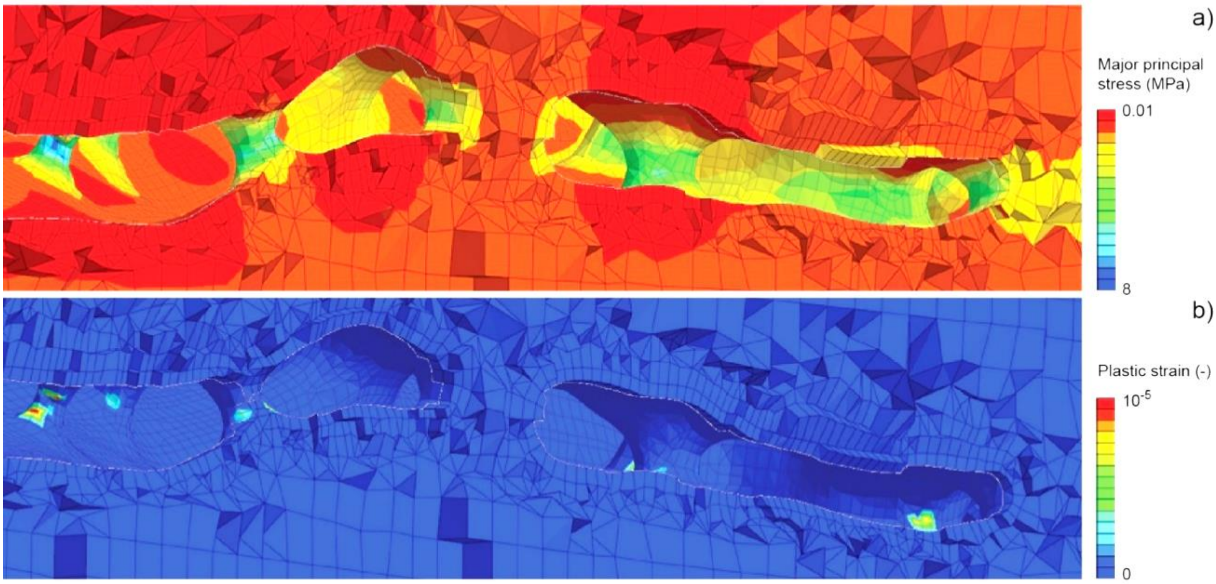

Figure 5. Detail of the mine-scale FE model results (upper mining level). a) distribution of major principal stress (σ_1); b) plastic strain outlining critical spots potentially affecting mine stability.

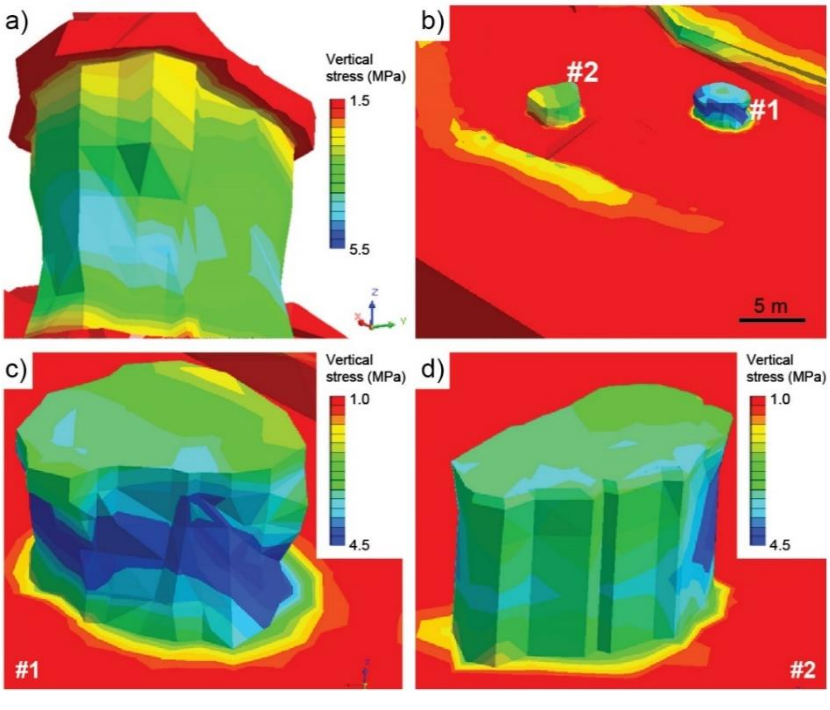

Figure 6. Local-scale modeling of individual pillars. a) distribution of vertical stresses as a function of pillar geometry; b) identification of stressed pillars in the global, mine-scale FEM 3D model; c) and d) analysis of selected pillars.

6. Conclusions

Our research showed that a realistic and optimized representation of 3D geometry is key to a meaningful assessment of the safety conditions of abandoned mines. Integrating modern high-resolution 3D survey technology within 3D numerical models provides powerful tools to analyze stress distributions and stability conditions, supporting a safe reuse of abandoned mining assets. Highly detailed representations of fine irregularities of roofs and pillars allow identifying critical spots, whose failure can potentially hamper global stability if strength reductions occur by progressive damage or weathering. On the other hand, numerical local failures can lead to underestimated global factors of safety, that must always be carefully interpreted in terms of mechanisms.

Acknowledgments
The authors thank the Municipality and local community of Dossena for supporting the research. We are indebted with Gexcel s.r.l. for providing Heron point clouds, and with Eng. P. Greco for his contribution to 3D solids for meshing. We also thank R. Milesi and F. Riva for they field support.

References
[1] Peila D, Pelizza S 1995 Civil reuses of underground mine openings: a summary of international experience *Tunn. Undergr. Sp. Tech.* **10**(2) 179-191
[2] Castellanza R, Nova R, Orlandi G 2010 Evaluation and remediation of an abandoned gypsum mine *J. Geotech. Geoenv. Eng.* **136**(4) 629-639
[3] Al Heib M, Duval C, Theoleyre F, Watelet JM, Gombert P 2015 Analysis of the historical collapse of an abandoned underground chalk mine in 1961 in Clamart (Paris, France) *Bull. Eng. Geol. Env.* **74**(3) 1001-1018
[4] Hajiabdolmajid V, Kaiser P 2003 Brittleness of rock and stability assessment in hard rock tunneling *Tunn. Undergr. Sp. Tech.* **18**(1) 35-48
[5] Vyazmensky A, Elmo D, Stead D 2010 Role of rock mass fabric and faulting in the development of block caving induced surface subsidence *Rock Mech. Rock Eng.* **43**(5) 533-556
[6] Lee SJ, Choi SO 2019 Analyzing the Stability of Underground Mines Using 3D Point Cloud Data and Discontinuum Numerical Analysis *Sustainability* **11**(4) 945
[7] Elmo D, Stead D 2010 An integrated numerical modelling–discrete fracture network approach applied to the characterisation of rock mass strength of naturally fractured pillars *Rock Mech. Rock Eng.* **43**(1) 3-19
[8] Hatzor YH, Talesncik M, Tsesarsky M 2002 Continuous and discontinuous stability analysis of the bell-shaped caverns at Bet Guvrin, Israel *Int. J. Rock Mech. Min. Sci.* **39** 867–886
[9] Ferrero AM, Segalini A, Giani GP 2010 Stability analysis of historic underground quarries. *Comp. Geotech.* **37**(4) 476-486
[10] Castellanza R, Orlandi GM, Di Prisco C, Frigerio G, Flessati L, Merodo JF, Agliardi F, Grisi S, Crosta GB 2015 3D numerical analyses for the quantitative risk assessment of subsidence and water flood due to the partial collapse of an abandoned gypsum mine. In *IOP Conference Series: Earth and Environmental Science* 26(1) 012058
[11] Fazio NL, Perrotti M, Lollino P, Parise M, Vattano M, Madonia G, Di Maggio C 2017 A three-dimensional back-analysis of the collapse of an underground cavity in soft rocks *Eng. Geol.* **228** 301-311
[12] Hoek E, Carranza-Torres C, Corkum B 2002 Hoek-Brown failure criterion-2002 edition *Proceedings of NARMS-Tac* **1**(1) 267-273
[13] Zlot R, Bosse M 2014 Efficient large-scale three-dimensional mobile mapping for underground mines *Journal of Field Robotics* **31**(5) 758-779
[14] García-Luna R, Senent S, Jurado-Piña R, Jimenez R 2019 Structure from Motion photogrammetry to characterize underground rock masses: Experiences from two real tunnels *Tunnelling and Underground Space Technology* **83** 262-273
[15] Dawson EM, Roth WH, Drescher A 1999 Slope stability by strength reduction *Geotechnique* **49** (6) 835–840
[16] Obert L, Duvall WI 196 Rock mechanics and the design of structures in rock J. Wiley, New York.